

THERMOELECTRIC PROPERTIES OF Ba-K-Si-Ca-P-O

W. Detkunthong, A. Dawongsa, P. Pilasuta and W. Somkhunthot*

Physics Department, Faculty of Science, Loei Rajabath University, Loei 42000, Thailand

Received 10 August 2012; Revised 30 October 2012; accepted 15 December 2012

ABSTRACT

The mineral samples were prepared to study the thermoelectric properties such as charge carrier, Seebeck coefficient, electrical resistivity, and thermal conductivity at room temperature in air. Charge carrier and Seebeck coefficient were measured by the hot probe method. Electrical resistivity can be determined from current-voltage characteristics. The steady state technique is used to find the thermal conductivity. Hot probe test found that the bulk sample presented n-type conduction. The Seebeck coefficient decreased with increasing the temperature of sintering. While the electrical resistivity and thermal conductivity increased. The measurements of thermoelectric properties showed the low Seebeck coefficient, high electrical resistivity, and the large thermal conductivity, which led to the low power factor and figure of merit. However, the mineral sample can convert thermal energy into electricity, which can be used to make the thermoelectric device.

KEYWORDS: thermoelectric properties, Ba-K-Si-Ca-P-O compound

* Corresponding authors; e-mail: weerasak1963@yahoo.co.th, Tel.: 66-08-17089677, Fax: 0-42835238

INTRODUCTION

Thermoelectric materials can convert thermal energy into electricity and electrical energy into cold. The good materials depend on their thermoelectric properties such as the Seebeck coefficient (S) [1, 2, 3], electrical resistivity (ρ) [4, 5, 6], and thermal conductivity (κ) [2, 7, 8]. For the thermoelectric efficiency can be calculated from the physical parameters S , ρ and κ such as the power factor ($P = S^2/\rho$) [2, 9] and figure of merit ($Z = S^2/\rho\kappa$) [10]. The development of thermoelectric materials will include the high S , low ρ and κ , which lead to the large P and Z . Besides, the thermoelectric performance of the materials is usually characterized in terms of their dimensionless figure of merit ($ZT = S^2T/\rho\kappa$, where T is the absolute temperature) [2, 9]. Namely, the large ZT values will be led to the high thermoelectric efficiency. Materials for thermoelectric energy conversion are two recognized the types of charge carriers such as n-type and p-type, which can be determined by hot probe technique [11, 12]. There are metals, semiconductors, and insulators, which have the Z values of $\sim 3 \times 10^{-6} \text{ K}^{-1}$, $\sim 2 \times 10^{-3} \text{ K}^{-1}$, and $\sim 5 \times 10^{-17} \text{ K}^{-1}$ at 300 K, respectively [13].

The search for new thermoelectric material is important that the metal oxide compounds were interested. The main objective of this study was

the thermoelectric properties of Ba-K-Si-Ca-P-O compound. It is the mineral at Ban Chiang Klom, Tambon Chiang Klom, Amphoe Pak Chom, which is located in the northern part of Loei Province, northeastern Thailand.

MATERIALS AND METHODS

The mineral samples were prepared to study the thermoelectric properties as shown in Figure 1. The mineral specimen was crushed and calcined at 500-900°C in air for 6 h. Each calcined powder precursors were crushed and mixed with PVA (polyvinyl alcohol) in 1 g:1 mL ratios and annealed at 100°C for 1 h in air. The calcined powders were then pressed into the bulk precursors at the pressure of 500 MPa in air before subjected to sintering stage. The bulk precursors were sintered at 600-1000°C in air for 6 h. Subsequently, the sintered bulks were cut and polished using the precision saw and grinder (IsoMet Low Speed Saw and MetaServ 3000, Buehler Ltd., USA). The dimension and density of sintered bulk samples are given in Table 1.

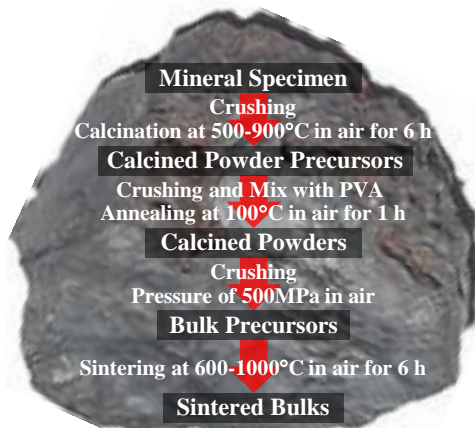


Fig. 1. Mineral and preparation of samples

Table 1. Dimension and density of the samples

Sintered Bulk Samples	Dimension			
	Width (mm)	Thickness (mm)	Length (mm)	Density (g/cm ³)
Non	3.80	3.10	20.10	2.55
at 600°C	3.95	3.82	17.65	2.24
at 700°C	3.80	3.60	20.18	2.05
at 800°C	4.07	3.08	19.85	2.38
at 900°C	3.91	3.05	20.24	2.55
at 1000°C	3.64	3.08	20.14	2.90

The mineral composition was analyzed using X-ray fluorescence spectrometry (Philips, Magix WDXRF). The identification of the samples were obtained from X-ray diffractometer (XRD-6100, Shimadzu using CuK α radiation, $\lambda = 1.5406 \text{ \AA}$).

The thermoelectric properties measurements included the charge carrier, Seebeck coefficient, electrical resistivity, and thermal conductivity at room temperature (T_{room}) in air. The experimental setups can be elucidated as follows.

Firstly, type of charge carrier and Seebeck coefficient (S) were measured by hot probe method [11] as shown in Figure 2(a). The hot and cold junctions between the across two ends of sample are connected to the digital voltmeter. The hot (T_H) and cold (T_C) temperatures are sensed by the type K thermocouples. The resistor (40 W 3.3 Ω) was used to heat the hot junction T_H by applying constant currents to the resistor placed on the hot side using the direct current power supply. The cold junction T_L was surrounded by air at room temperature. Seebeck coefficient was measured by the relation between thermoelectric voltage (ΔV) and temperature difference ($\Delta T = T_H - T_C$). The S is defined as [2]:

$$S = \frac{\Delta V}{\Delta T} \quad (1)$$

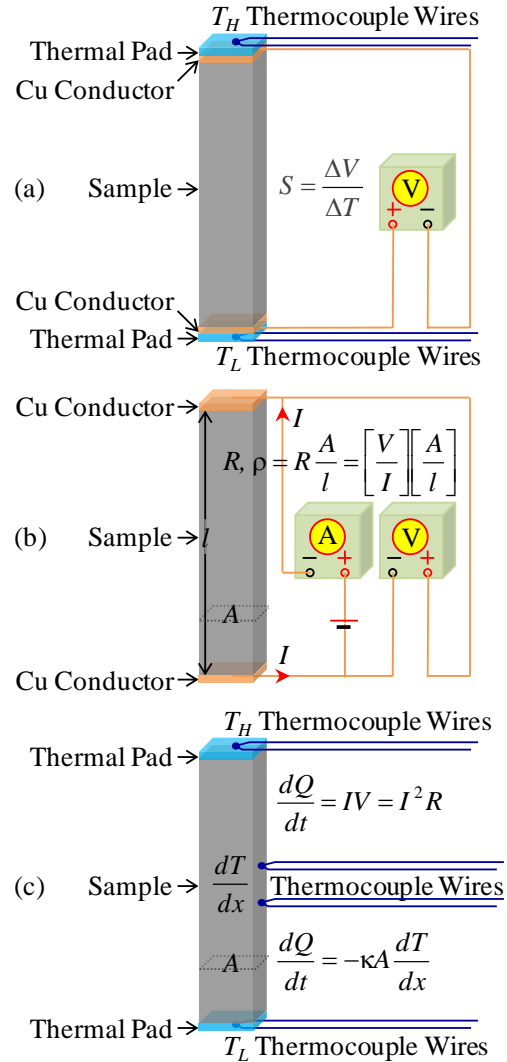


Fig. 2. Thermoelectric properties measurements

Secondly, electrical resistivity (ρ) can be determined from current-voltage characteristics [4] as shown in Figure 2(b). The direct current power supply was used by applying the currents to sample. The current (I) and voltage (V) are measured. The ρ can be estimated from [4]:

$$\rho = \left[\frac{V}{I} \right] \left[\frac{A}{l} \right] \quad (2)$$

where A and l are the cross-sectional area and length of the bulk sample, respectively.

Thirdly, the steady state technique is used to find the thermal conductivity (κ) [2] as shown in Figure 2(c). The heat flow rate (dQ/dt) between two ends of the solid can be given as [8]:

$$\frac{dQ}{dt} = -\kappa A \frac{dT}{dx} \quad (3)$$

where $dQ/dt = IV = I^2R$ is directly proportional to the cross-sectional area A . The I and V is the current and voltage to the resistance R , which was used to heat the hot junction by applying constant currents to the resistor (40 W 3.3 Ω) placed on the hot side using the direct current power supply. dT/dx is the temperature gradient along the path of the heat flow. The T_H , T_C , and dT are sensed by the type K thermocouples.

Finally, the thermoelectric efficiency can be examined from the power factor (P) and figure of merit (Z). The P was calculated from the S and ρ in Equation (4) [2, 9],

$$P = \frac{S^2}{\rho} \quad (4)$$

The performance of thermoelectric materials is usually characterized in terms of their figure of merit parameter in Equation (5) [10],

$$Z = \frac{S^2}{\rho\kappa} \quad (5)$$

RESULTS AND DISCUSSION

The composition of the crushed mineral was analyzed using XRF. The concentrations (%) of elements and compounds are given in Table 2. The result indicated that the concentrations of barium (Ba), potassium (K), oxygen (O), silicon (Si), calcium (Ca), and phosphorus (P) contents in the crushed mineral were 35.47, 25.32, 23.92, 9.79, 4.09, and 1.41%, respectively. The crushed mineral included barium oxide (BaO) 39.60%, potassium oxide (K₂O) 30.51%, silicon dioxide (SiO₂) 20.93%, calcium oxide (CaO) 5.72%, and diphosphorus pentoxide (P₂O₅) 3.24%. Hence, it can be exhibited that the mineral sample will contain these species composition. From this point onward, the mineral sample will be referred to as Ba-K-Si-Ca-P-O containing.

The identification of the samples were obtained from XRD, which were measured in the 2-theta angle range of $20^\circ \leq 2\theta \leq 80^\circ$ with scanning rate of 0.02°/sec. XRD pattern is shown in Figure 3. The samples were composed of the BaO, K₂O, SiO₂, CaO, P₂O₅, and K phases.

The XRF and XRD results showed that the mineral sample comprised the Ba-K-Si-Ca-P-O compound.

The measurement results of thermoelectric properties of bulk samples such as the type of charge carrier, Seebeck coefficient, electrical

resistivity, and thermal conductivity are presented and discussed.

Table 2. Composition of mineral sample

Concentrations (%)						
Ba	K	O	Si	Ca	P	Total
35.47	25.32	23.92	9.79	4.09	1.41	100
BaO	K ₂ O	SiO ₂	CaO	P ₂ O ₅	-	Total
39.60	30.51	20.93	5.72	3.24		100

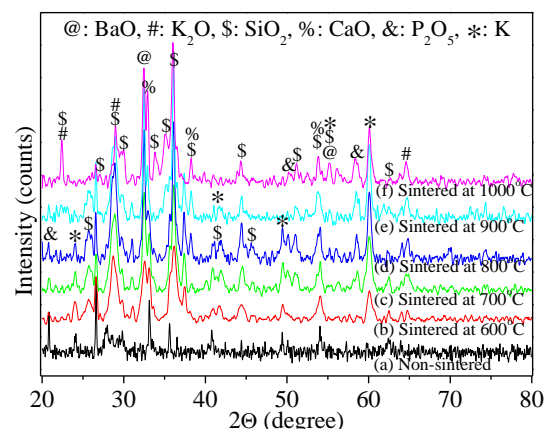


Fig. 3. XRD pattern of mineral samples

Firstly, the measured results of charge carrier demonstrated that the hot junction shows higher voltage than the cold junction, indicating that the electrons conduction dominated the transport properties (n-type). The relation between the thermoelectric voltage and temperature difference at room temperature in air are shown in Figure 4(a). The Seebeck coefficient indicated linear dependence between the thermoelectric voltage and temperature difference. The $|S|$ of 0.20 ± 0.01 mV/K is obtained for the non-sintered bulk sample, and decreased with increasing the temperature of sintering from 0.18 ± 0.02 mV/K at 600°C to 0.08 ± 0.01 mV/K at 1000°C.

Secondly, the experimental results of I - V characteristics at room temperature in air are shown in Figure 4(b). It can be seen that the plot exhibit a good ohmic I - V characteristics. The ρ of 1.42 ± 0.15 k Ω -m is attained for the non-sintered bulk sample, and increased with increasing the temperature of sintering from 1.69 ± 0.07 k Ω -m at 600°C to 3.92 ± 0.32 k Ω -m at 1000°C.

Thirdly, the relative results of heat flux and temperature gradient at room temperature in air are shown in Figure 4(c).

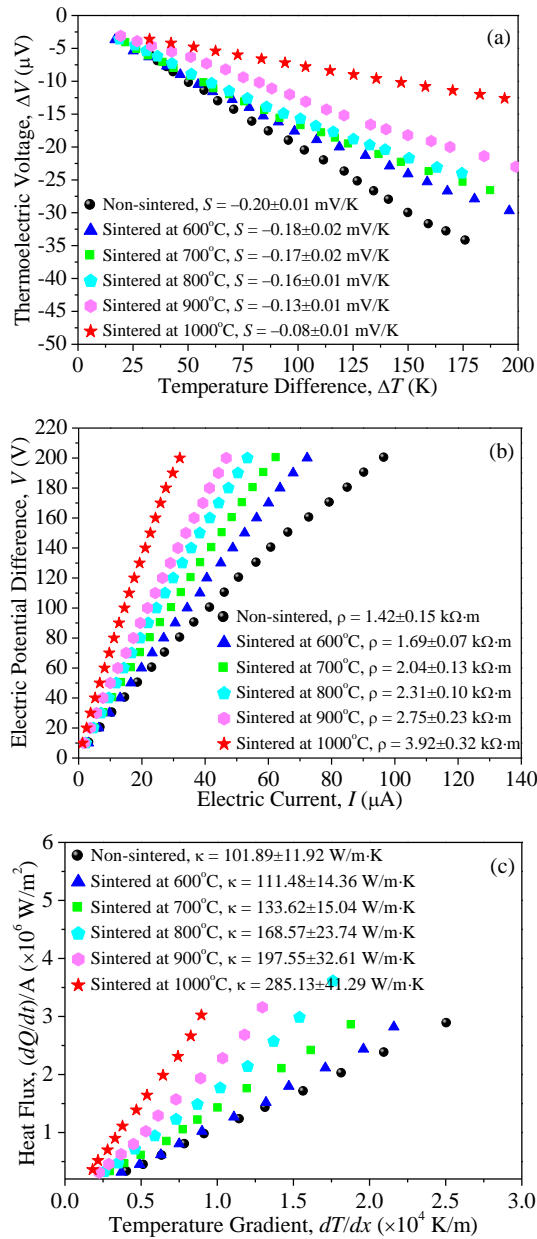


Fig. 4. Results of thermoelectric properties

The κ of 101.89 ± 11.92 W/m-K is achieved for the non-sintered bulk sample, and increased with increasing the temperature of sintering from 111.48 ± 14.36 W/m-K at 600°C to 285.13 ± 41.29 W/m-K at 1000°C.

Finally, the power factor and figure of merit were calculated. The values of S , ρ , κ , P , and Z are summarized in Table 3. The results give the P and Z values of $(2.82 \pm 0.58) \times 10^{-11}$ W/m-K 2 and $(2.76 \pm 0.89) \times 10^{-13}$ K $^{-1}$, for the non-sintered bulk sample, and increased with increasing the temperature of sintering, respectively. The sintered bulk samples showed the low S , high ρ , and large κ , which led to the low P and Z .

CONCLUSION

The XRF and XRD results showed that the mineral sample comprised the Ba-K-Si-Ca-P-O compound. The measurement results of thermoelectric properties found that the bulk samples showed the low Seebeck coefficient, high electrical resistivity, and large thermal conductivity, which led to the low power factor and figure of merit. However, the mineral sample can convert thermal energy into electricity, which can be used to make the thermoelectric device.

ACKNOWLEDGEMENTS

This work was financially supported by the Research and Development Institute, Loei Rajabhat University. Asst.Dr.Tosawat Seetawan, the Thermoelectric Research Center, Sakon Nakhon Rajabhat University, Thailand are gratefully acknowledged for the preparation of the samples. The Physics Department, Faculty of Science, Ubon Rajathane University is acknowledged for the XRF and XRD analysis.

Table 3. S , ρ , κ , P , and Z of Ba-K-Si-Ca-P-O compound at room temperature in air

Bulk Samples	S (mV/K)	ρ (k $\Omega\cdot\text{m}$)	κ (W/m-K)	P ($\times 10^{-11}$ W/m-K 2)	Z ($\times 10^{-13}$ K $^{-1}$)
Non-sintered	-0.20 ± 0.01	1.42 ± 0.15	101.89 ± 11.92	2.82 ± 0.58	2.76 ± 0.89
Sintered at 600°C	-0.18 ± 0.02	1.69 ± 0.07	111.48 ± 14.36	1.92 ± 0.51	1.72 ± 0.67
Sintered at 700°C	-0.17 ± 0.02	2.04 ± 0.13	133.62 ± 15.04	1.42 ± 0.42	1.06 ± 0.44
Sintered at 800°C	-0.16 ± 0.01	2.31 ± 0.10	168.57 ± 23.74	1.11 ± 0.19	0.66 ± 0.20
Sintered at 900°C	-0.13 ± 0.01	2.75 ± 0.23	197.55 ± 32.61	0.61 ± 0.15	0.31 ± 0.13
Sintered at 1000°C	-0.08 ± 0.01	3.92 ± 0.32	285.13 ± 41.29	0.16 ± 0.05	0.06 ± 0.03

REFERENCES

- [1] Yunus, C. and Boles, M. Thermodynamics: an engineering approach. Hightstown, McGraw Hill, 1998.
- [2] Nolas, G.S., Sharp, J. and Goldsmid, H.J. Thermoelectrics, basic principles and new materials developments. Berlin, Springer-Verlag, 2001.
- [3] http://en.wikipedia.org/wiki/Thermoelectric_effect
- [4] Schroder, D.K. Semiconductor material and device characterization. 3 rd ed. New Jersey, John Wiley & Sons 2006.
- [5] [http://www.michaelburns.net/Info/Resisitvity%20Measurement%20\(MICE%20excerpt\).pdf](http://www.michaelburns.net/Info/Resisitvity%20Measurement%20(MICE%20excerpt).pdf)
- [6] http://www.physics.sjsu.edu/becke/physics51/dc_circuits.htm
- [7] <http://mathworld.wolfram.com/HeatConductionEquation.html>
- [8] Marion, J.B. and Hornyak, W.F. General physics with bioscience essays. 2 nd ed. New York, John Wiley & Sons, 1985.
- [9] Rowe, D.M. CRC handbook of thermoelectrics. Boca Raton, FL, CRC Press, 1995.
- [10] Altenkirch, E. Electrotehrmische Kalteerzeugung und Reversible Elektrische Heizung, Physikalische Zeitschrift, 12, 1911, 920-924.
- [11] <http://ecee.colorado.edu/~bart/book/book/contents.htm>
- [12] <http://www.tellurex.com/pdf/peltier-faq.pdf>
- [13] Wood, C. Materials for Thermoelectric Energy Conversion. Report on Progress in Physics